NeuroToxicology 58 (2017) 226–237

Contents lists available at ScienceDirect

NeuroToxicology

Full Length Article

The application of PBPK models in estimating human brain tissue manganese concentrations

Siva P. Ramoju[a,*], Donald R. Mattison[a,b], Brittany Milton[a], Doreen McGough[c], Natalia Shilnikova[a,b], Harvey J. Clewell[d], Miyoung Yoon[d], Michael D. Taylor[e], Daniel Krewski[a,b], Melvin E. Andersen[d]

[a] Risk Sciences International, 55 Metcalfe Street, Suite 700, K1P 6L5, Ottawa, Canada
[b] Samuel R. McLaughlin Centre for Population Health Risk Assessment, Faculty of Medicine, 850 Peter Morand Crescent, Room 119, University of Ottawa, Ottawa, K1G 3Z7, Canada
[c] International Manganese Institute, 17 rue Duphot, 75001 Paris, France
[d] ScitoVation, 6 Davis Drive, PO Box 110566, Research Triangle Park, NC 27709,United States
[e] Nickel Producers Environmental Research Association (NiPERA), 2525 Meridian Parkway, Suite 240, Durham, NC 27713, United States

ARTICLE INFO

Article history:
Received 5 July 2016
Received in revised form 1 December 2016
Accepted 1 December 2016
Available online 15 December 2016

Keywords:
Manganese risk assessment
PBPK models
Neurotoxicity
Categorical regression

ABSTRACT

Mn is an essential element that causes neurotoxicity in humans when inhaled at high concentrations. This metal has well-recognized route-dependent differences in absorption, with greater proportionate uptake for inhalation versus dietary exposure. Physiologically-based pharmacokinetic (PBPK) models for Mn have included these route specific differences in uptake and their effect on delivery of Mn to target tissues via systemic circulation. These PBPK models include components describing ingestion and inhalation, homeostatic control (concentration dependent biliary elimination and gastrointestinal absorption), and delivery to target sites within the brain. The objective of this study was to combine PBPK modeling of target tissue Mn concentration and categorical regression analysis to identify Mn intake levels (both by food and air) that are expected to cause minimal toxicity. We first used the human PBPK model to describe blood Mn data from three occupational exposure studies, demonstrating consistency between model predictions and measured data. The PBPK model was then used to predict concentrations of Mn in the globus pallidus (the presumed target tissue for motor function disruption in humans) for various epidemiological studies. With the predicted globus pallidus concentration of Mn, we conducted categorical regression modeling between globus pallidus Mn and severity-scored neurological outcome data from the human cohorts. This structured tissue dose – response analysis led to an estimated 10% extra risk concentration (ERC_{10}) of 0.55 μg/g Mn in the globus pallidus, which is comparable to similar values estimated by the Agency of Toxic Substances and Disease Registry and Health Canada (after translation from external exposure to tissue dose). The steep dose-response curve below this ERC_{10} value may be used to inform the choice of adjustment factor to translate the ERC_{10} as a point of departure to a reference concentration for occupational or environmental exposure to Mn. Because these results are based on human epidemiological data and a human PBPK model, adjustment or translation of results from animals to humans is not required.

1. Introduction

Manganese (Mn) is an essential nutrient for humans, with the main source of intake being dietary. Given its abundance in food, Mn deficiency is uncommon. Excess oral Mn exposures are mitigated in part by the body's natural ability to regulate dietary absorption and elimination. However, high oral exposure levels are reported to cause neurological effects in human populations that consumed water or food with total Mn intakes of more than 10 mg Mn/d (Iwami et al., 1994; Kondakis et al., 1989; Ljung and Vahter, 2007; O'Neal and Zheng, 2015). Humans are also exposed through inhalation of airborne Mn particles from a variety of environmental and occupational sources. In occupations such as Mn alloy production (ferromanganese and silicomanganese), welding, Mn metals and dry cell battery manufacture, workers may be exposed to Mn dust and fumes (ATSDR, 2012). Due to its ability to bypass

* Corresponding author.
E-mail address: sramoju@risksciences.com (S.P. Ramoju).

http://dx.doi.org/10.1016/j.neuro.2016.12.001
0161-813X/

liver-mediated elimination, high levels of inhaled Mn are known to accumulate in some brain regions leading to neurological impairment. Short-term exposure to high levels of Mn are reported to induce portal of entry effects such as breathing discomfort, as well as systemic responses in the central nervous systems such as headaches, mood changes, and sleeplessness. Depending on exposure concentration and duration, the health outcomes reported in Mn industry workers at lower exposure levels range from subtle and subclinical changes, such as poor performance in various neurobehavioral tests, to overt clinical signs, such as altered gait, muscle weakness, mild tremors, postural instability and various psychiatric disturbances, collectively termed 'manganism' (Bowler et al., 2006; Guilarte, 2010; O'Neal and Zheng, 2015; Perl and Olanow, 2007). Environmental exposures, in addition to fugitive dusts from nearby industries, include exposure to low levels of Mn through combustion products of the anti-knock gasoline additive methylcyclopentadienyl Mn tricarbonyl (MMT) and Mn-containing fungicides such as Mancozeb and Maneb (ATSDR, 2012; Gunier et al., 2014).

1.1. Pharmacokinetics of manganese

Ingestion and inhalation are the main routes of Mn intake; dermal intake of Mn is essentially negligible (ATSDR, 2012). Dietary Mn intake varies depending on the solubility of the Mn salt, but is generally low, ranging between 3 and 5% (Aschner and Aschner, 2005; Davis et al., 1993; Finley et al., 1994). The bioavailability of inhaled Mn depends on the form of Mn as well as the size of the inhaled particles. Small sized particles – considered as 'respirable' – can penetrate into the lower regions of the lung and have greater pulmonary absorption. Relatively large (coarse) particles deposit either in the head (nasal cavity and mouth) or upper respiratory region and are subsequently moved up to the trachea; particles moving up through the trachea are swallowed into the gastrointestinal tract. Among various Mn salts, chloride and sulfate salts are the most soluble (and hence the most bioavailable), while oxides are sparingly soluble (Dorman et al., 2001). The most abundant naturally occurring Mn salts are oxides (MnO_2 and Mn_3O_4) found in minerals and soils (Post, 1999).

Tissue distribution (influx and efflux) of Mn is mediated primarily by transporter (importers and exporters) proteins. Among the various available importers, 'divalent metal transporter 1' (DMT1) is the primary transporter of divalent ions with greater affinity for Mn than Fe and is responsible for transportation of Mn^{2+} ions from blood to brain through the blood-brain-barrier (Aschner et al., 2007; Chen et al., 2015; O'Neal and Zheng, 2015). These transporters are abundant in certain regions of the brain such as the globus pallidus and basal ganglia, which may explain the differential accumulation of Mn in these brain regions compared to others (Aschner et al., 2009, 2007). Another important influx transporter is the trivalent ion carrier called 'transferrin' (Tf), note that Tf also transports Fe, leading to Mn-Fe interactions in uptake (O'Neal and Zheng, 2015). Tf is mostly found in blood plasma and is responsible for the transfer of Mn^{3+} ions from blood to cells, where Mn^{3+} ions are reduced to divalent ions prior to uptake by mitochondria (Gunter et al., 2013). In addition, Fe and Mn can compete for the Iron Regulatory Protein-1 (IRP1) (O'Neal and Zheng, 2015). The efflux of Mn is a comparatively less studied process. Recently the protein products of genes *SLC30A10* and *ATP13A2* as well as the iron transporter ferroportin have been identified as Mn efflux transporters (Chen, 2015; Tan et al., 2011). Mutations in *SLC30A10* lead to Parkinsonian-like gate disturbances and hypermanganesemia in humans, reflecting the importance of this gene product in Mn homeostasis (DeWitt et al., 2013).

Each tissue contains some level of Mn; tissues rich in mitochondria and pigments have relatively high basal Mn levels. In general, Mn has comparatively higher concentrations in the liver, brain and bone tissue than in other tissues. Rodent and primate inhalation exposure studies have demonstrated that brain tissues showed higher partitioning compared to other tissues (Dorman et al., 2004, 2006; Normandin et al., 2002; Salehi et al., 2003). Further, Mn exhibits preferential uptake within various brain regions. Brain magnetic resonance imaging (MRI) investigations of Mn-exposed workers found a higher pallidal index relative to healthy subjects, indicative of higher levels of Mn in the globus pallidus than in other brain regions (Jiang et al., 2007; Kim et al., 2005; Li et al., 2014). X-ray fluorescence imaging studies (XRF) demonstrates that regions of the brain containing high levels of Fe also contain high levels of Mn (O'Neal and Zheng, 2015). Similarly, pathological evaluations in patients with manganism found consistent damage in the globus pallidus across all these patients, consistent with Mn-induced neurotoxicity (Perl and Olanow, 2007). In addition, Mn exposure has been demonstrated to alter neurotransmitter and metabolite concentrations, including dopamine, dopamine metabolites, such as 3,4-dihydroxyphenylacetic acid (DOPAC) and homovanillic acid (HVA), and GABA, in rat brain. Suggesting alterations in neurotransmitters rather than dopaminergic neurons (O'Neal and Zheng, 2015). Typically, background levels of Mn in human brain range between 0.3–0.7 μg/g of wet tissue (Douglas et al., 2010).

The primary elimination pathway of Mn is biliary elimination. Mn becomes concentrated in the bile and is moved into the small intestine where it is subsequently excreted primarily in feces; relatively small amounts are eliminated through urine (Crossgrove and Zheng, 2004; Davis et al., 1993; Malecki et al., 1996). Inducible biliary elimination in conjunction with controlled gut uptake (a homeostatic mechanism) regulates Mn levels in the body (i.e. by reducing absorption from the gut and increasing the rate constant for elimination in bile). Brain tissues show slower clearance rates than liver or kidney tissues (Crossgrove and Zheng, 2004). In humans, the half-life of Mn is tissue dependent. Following intravenous ^{54}Mn tracer injections, the half-life for whole-body clearance is 37.5 days and for the head, including bone, is 54 days (Cotzias et al., 1968).

1.2. Mn PBPK model for humans

The main goal of constructing a physiologically based pharmacokinetic (PBPK) model of Mn is to facilitate quantitative estimation of Mn disposition in specific target tissues resulting from both oral and inhalation routes of exposures, while accounting for both essentiality and toxicity of Mn. To this end, PBPK models were developed, tested against data from human subjects, and validated to assess health risks related to integrated exposures to Mn through multiple routes, based upon a series of pharmacokinetic experiments involving both inhaled and oral Mn (Andersen et al., 2010; Leavens et al., 2007; Nong et al., 2009, 2008; Schroeter et al., 2011; Teeguarden et al., 2007a, 2007b, 2007c). It's important to note that these models are developed to account for body burdens from systemic circulation of Mn through the blood as well as direct transfer via the olfactory pathway, although the contribution of this pathway for delivery to target tissues within the midbrain is considered relatively insignificant (Leavens et al., 2007).

PBPK models were first developed for adult rats, subsequently extrapolated to monkeys, and then to humans. These PBPK models have liver, lung, nasal cavity, bone, blood, and brain compartments, which are interconnected by the blood compartment. The brain is further divided into four regions representing globus pallidus, cerebellum, pituitary gland, olfactory bulb and brain blood (Fig. 1). Remaining body tissues are combined into a single compartment – 'rest of body'. In-depth characterizations of

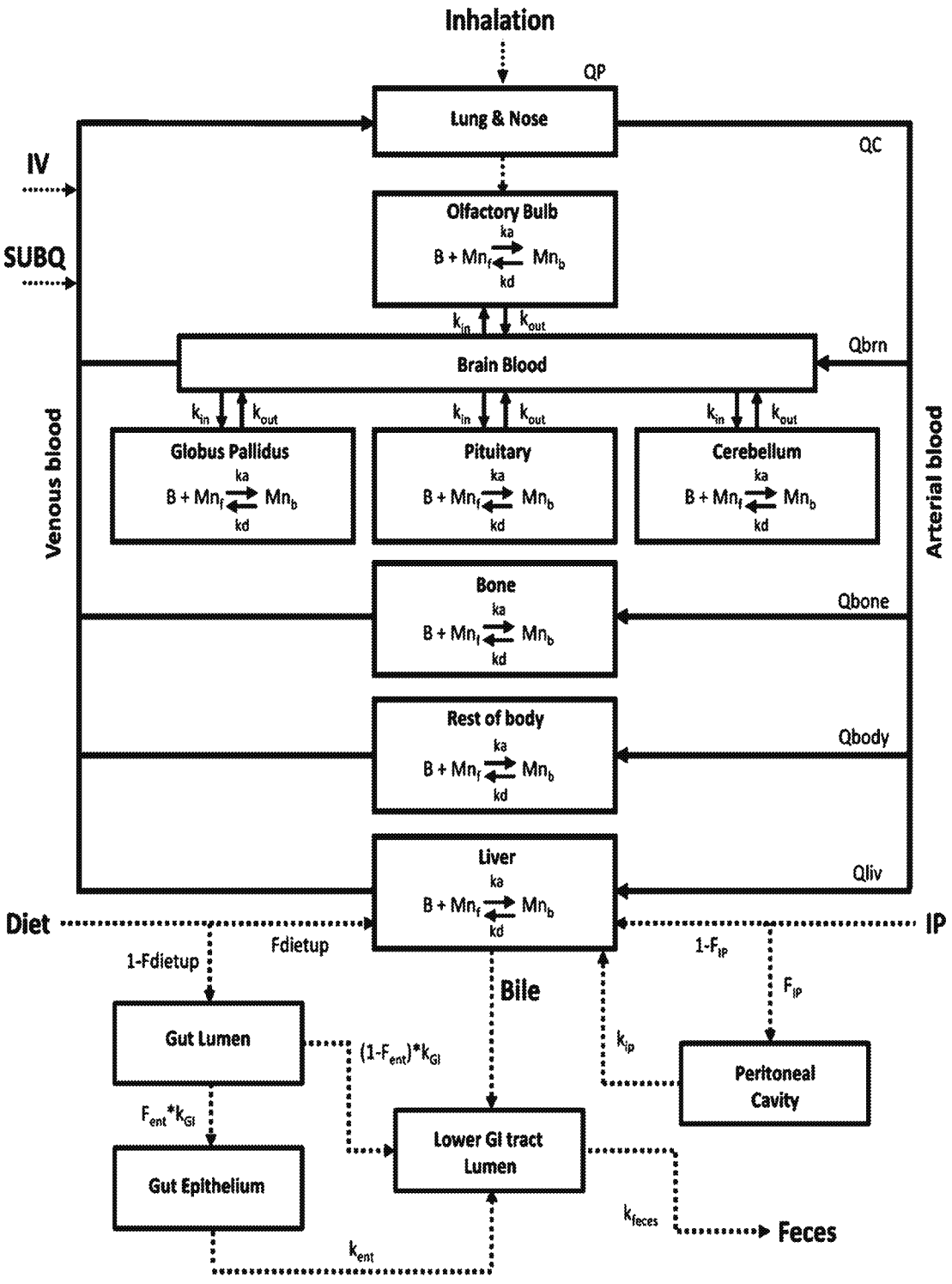

Fig. 1. Human PBPK model structure describing the Mn pharmacokinetics in various tissue compartments, as shown in of Schroeter et al. (2011). In each compartment, B: tissue binding capacity, Mnf: free Mn, Mnb: bound Mn, Ka & kd: association and dissociation rate constants, kin and kout: influx and efflux diffusion rate constants, QP, QC, and Qtissue: pulmonary ventilation, cardiac output, and tissue blood flows; Fdietup: fractional gut absorption; Fent: fractional enterocyte storage; Fip: fractional IP dose absorption constant; kGI: transfer rate from gut lumen; kent: enterocyte sloughing rate; kfeces: elimination rate constant through feces; kIP: transfer rate from peritoneal cavity to liver.

various physiological parameters for these models and technical details of model development including uncertainty analysis are described elsewhere (Nong et al., 2009, 2008; Schroeter et al., 2011; Taylor et al., 2012).

The underlying biological mechanisms of these models are as follows: Mn absorbed via food or air or water is distributed in the body as free Mn and is bound to tissues (known as compartments for modeling purposes); levels of bound Mn are determined by tissue specific binding rate constants (association and dissociation rate constants; k_a and k_d, respectively) and binding capacities; differential diffusion (influx and efflux rate constants) is maintained across various tissues (such as preferential increase of Mn in

certain tissues under high inhalation exposure conditions); and, most importantly, a robust homeostatic mechanism is in place through dietary absorption and biliary elimination to maintain the basal tissue Mn levels for dietary intakes. Under normal conditions (dietary exposure only and with no or minimal inhalation exposures), basal tissue Mn is mostly in the bound form (for example, the fraction of bound Mn in the human brain is around 80%). Under excess inhalation exposure conditions, with saturation of homeostatic controls (dose-dependent biliary elimination and tissue binding capacities), free Mn levels in various tissues start to disproportionately increase (Schroeter et al., 2011).

The PBPK models indicate that a nonlinear relationship exists between increases in Mn in air (MnA) and globus pallidus Mn (MnGP), and that an increase in MnGP above basal concentrations is expected when air Mn levels increase above 10–100 μg Mn/m^3 (Taylor et al., 2012). Clinically, use of magnetic resonance imaging (MRI) and spectroscopy (MRS) allow assessment of Mn concentrations in the brain as well as neurotransmitter levels providing non-invasive information on exposure-response relationships with respect to central nervous system toxicity (O'Neal and Zheng, 2015).

1.3. Objectives

Increases in brain Mn especially in regions such as substantia nigra, globus pallidus and striatum occur in occupational and environmental exposure studies. Higher levels of Mn in these brain regions result in oxidative stress-mediated neuronal injury causing several neurological conditions associated with motor and cognitive functions, collectively termed 'manganism'. Symptoms of manganism include rigidity, tremor, dystonic movements and bradykinesia, similar to Parkinson's disease (PD) (Cersosimo and Koller, 2006; Guilarte, 2010; Olanow, 2004). MRI investigations suggest that globus pallidus is the primary site for increased Mn concentration in subjects occupationally exposed to Mn such as welders and smelter workers (Kim et al., 2005). Therefore, increases in Mn above normal levels in the globus pallidus should be the most relevant and sensitive metric for human health risk assessment. Our working hypothesis is that there is a threshold for Mn neurotoxicity related to the no-observed-adverse-effect-tissue-concentration (NOAEtC), or, equivalently, to the maximum air Mn concentration associated with NOAEtC, that avoids significant increases of Mn above basal levels in the globus pallidus. The objectives of the study are to identify the NOAEtC and the maximum air Mn concentration associated with it across multiple human epidemiological studies of manganese exposure using PBPK and categorical regression modeling.

2. Methods

Our methodological approach to characterizing tissue-dose response involved the following steps. First, occupational epidemiological studies with well-characterized exposures and outcomes were identified. Second, a PBPK model was used to estimate the increases in Mn in target tissues under the reported exposure conditions of selected studies. Third, a dose-response analysis was conducted using categorical regression (Milton et al., 2016) to establish the target tissue concentration corresponding to a minimal or negligible risk level (equivalent to the NOAEL) associated with health effects. Exposures (manganese in air) associated with this no-risk-tissue-dose can then be proposed as a safe reference value under given exposure conditions (whether ambient or occupational). Detailed information on the model and relevant physiological parameters is available at the following US EPA website: http://www.regulations.gov/, identified by docket number EPA-HQ-OAR-2004-0074.

2.1. Selection of human studies and assigning severity scores

Details on literature search methodology and inclusion/exclusion criteria for construction of a database for conducting a dose-response analysis (Categorical Regression analysis) of Mn-induced health effects were described by Mattison et al. (2017). In the present analysis, human occupational inhalation exposure studies focusing on understanding the relationship between well characterized Mn exposures and neurological manifestations were included (see Table 2 for a listing and characteristics of the studies). All studies were cross-sectional in nature.

2.2. PBPK modeling of human studies

The PBPK model is represented as a system of differential equations: solving these equations yields the time course (time versus concentration plots, as an example) of Mn in different tissues represented as compartments. A description of the model structure as well as the equations and constants associated with various kinetic processes is provided in Fig. 1. The complete computer code of the PBPK model was acquired from developers in its original form as described in the technical publication by Schroeter et al. (2011). The original PBPK model code was written in Advanced Computer Simulation Language (ACSL) and was executed as a .csl file; study-specific scripts were developed and edited in MatLab and executed as .m files. Both .m and .csl files were executed in the AcslXtreme software environment (version 3.0.2.1, Aegis Technologies Group, Inc., Huntsville, AL). All model parameter values were identical to those used in the published model.

2.3. Study-specific PBPK model inputs

For estimation of tissue levels using a PBPK model, the following exposure group specific inputs are required: Mn concentration and particle size distribution of the workplace environment, exposure duration, and lung deposition fractions of inhaled air. These inputs are described in more detail below.

2.3.1. Exposure concentration and duration

Average (arithmetic mean or AM) Mn concentration and average (AM) exposure durations of each exposure group as reported in the original publication were used. All air dust measurements were based on personal sampling. We considered Mn content only in the respirable dust fraction; respirable fractions as reported in the original publications were used.

2.3.2. Lung deposition fractions

Information on the size of dust particles inhaled and the breathing pattern of the subjects is necessary to understand the deposition of particles in different regions of the airways. Particle size distribution (PSD) of airborne dust is occupation- or workplace-specific (IEH, 2004), and appropriate PSD data is needed for estimating lung deposition fractions of the exposed workers. However, none of the selected studies reported particle size measurements of the workplace environment. We conducted a literature search and identified studies that reported PSDs based on personal cascade impactor measurements from workplaces similar to those in our selected studies. Based on these study reports, we collected occupation-specific PSD information either as reported, or made assumptions, where necessary. For simplicity, various tasks performed by subjects from selected studies were categorized into three types of occupations i.e. welders, ferroalloy production workers, and dry-cell battery workers. A list of PSD data (particulate mass median aerodynamic diameter or MMAD, and geometric standard deviation or GSD) of

Table 1
Particle size distribution (PSD) data of the three occupation types considered in the current analysis and respective MPPD model-derived (MPPD version 2.1, Applied Research Associates, Inc., NM) deposition fractions in various regions of the human respiratory tract.

Occupation Type	MPPD Model Inputs		Estimated Airway Deposition Factions[h]		
	MMAD[a]	GSD[b]	Head (H)	Tracheobronchial (TB)	Pulmonary (P)
Ferroalloy workers	2.6[c]	4.5[c]	61.8%	3.7%	7.3%
Welders	0.33[d]	4.0[d]	21.1%	9.8%	20%
	0.54[e]	2.4[e]	24.5%	6.6%	15.1%
Battery workers	5[f]	3[g]	82.4%	2.1%	6.1%

[a] MMAD = mass median aerodynamic diameter.
[b] GSD = geometric standard deviation.
[c] PSD data of particles in the size range of 0–10 μm collected in two ferroalloy smelters – as reported in Table 3 of Berlinger et al. (2011).
[d] PSD data of flux-cored arc welding (FCAW) fume particles (size range 0.4 to >5.8 μm) – as reported in Table 4 of Jenkins et al. (2005).
[e] PSD data of manual metal arc welding (MMAW) fume particles (size range 0.02–16 μm) – estimated based on Fig. 2 of Berlinger et al. (2011).
[f] Median cut point for the respirable dust fraction as reported in USEPA (1993) and Roels et al. (1999) battery worker study.
[g] assumed.
[h] MPPD model running conditions: Human Yeh/Schum symmetric lung + 20 breaths/min + 1.25 L tidal volume + oronasal-mouth breathing + inhalability adjustment OFF + remaining parameters were defaulted to the airway morphometry model.

each type of occupation, along with assumptions, where appropriate, is provided in Table 1.

Respiratory tract deposition fractions were estimated using the publicly available Multiple-Path Particle Dosimetry model (MPPD version 2.1, Anjilvel and Asgharian (1995), Applied Research Associates, Inc., NM). This model can be used to estimate deposition fractions in both human and rat airways for particles ranging from ultrafine (0.01 μm) to coarse (20 μm) particles (Asgharian et al., 2001). To run the MPPD model, species-specific lung geometries, ventilatory rates (specific to subject's activity level) and PSD of inhaled dust are required. The human Yeh/Schum symmetric lung model was selected as an airway morphometry model type. Light exercise with 20 breaths/min, 1.25 L tidal volume and oronasal-mouth breathing was assumed to represent activity level (ICRP, 1994). Since inhalability for respirable particles (< 10 μm) is around one, the inhalability adjustment was turned off (ICRP, 1994). Remaining parameters defaulted to the selected airway morphometry model. Table 1 summarizes the estimated deposition fractions (MPPD model outputs) in the head, tracheobronchial and pulmonary regions.

Other parameters such as exposure length (8 h/day & 5 days/week), basal diet Mn levels (3 mg/day, which is calculated from adequate daily intakes of 1.8–2.3 mg/day recommended for adults by Aschner and Aschner (2005)), and average body weight (70 kg) were held constant across all study simulations. Each study was simulated by running the model from the beginning of the exposure period (time = 0, including acclimatization period) to the end of exposure (here, the point at clinical outcomes were evaluated). For each study or exposure group, the tissue dose metric relevant for dose-response analysis – the globus pallidus Mn (MnGP) concentration at the end of exposure (EoE) – was collected. The parameter values of the PBPK model specific to each study are presented in Table 2.

2.4. PBPK modeling with exposed humans

The models were tested by simulating additional studies that reported whole blood Mn levels, and comparing the model-predicted blood Mn (MnB) levels with those experimentally measured in subjects from the same study. The first dataset used for validation was based on the data reported by Baker et al. (2014) who collected data on air Mn and blood Mn from 24 publications. For the present purposes, data on mean MnB and mean air Mn (MnA) of eight welder exposure groups identified by Baker et al. (Chang et al., 2010; Ellingsen et al., 2006; Jarvisalo et al., 1992; Pesch et al., 2012; Wang et al., 2006) were extracted. The second dataset was based on subjects employed in two ferroalloy plants (Apostoli et al., 2000). Individual data on air monitoring as reported in this study, used as model input (extracted from Fig. 4 of Apostoli et al. (2000)). The final dataset (Roels et al., 1987) included mean MnA levels in eleven workplaces at a Mn oxide and salt producing plant, and mean MnB levels of the workers at these workplaces. All three datasets contained multiple exposure levels allowing the model to be tested across a range of exposure concentrations.

2.5. Tissue dose – response analysis

A tissue dose – response analysis (regression analysis) was performed using the *CatReg* tool (version 2.3), a software program developed by the US Environmental Protection Agency (US EPA). A key feature of *CatReg* is its ability to analyze data and/or results from multiple studies simultaneously (USEPA, 2006). Combining information across multiple studies allows the users to consider both dose and duration as contributing factors when estimating toxicity. The dose – response curves provided by *CatReg* calculate the probability of severity as a function of dose and time. *CatReg* provides an estimate of the Extra Risk Concentration (ERC_q), defined as the dose, c, for which the probability of an adverse effect of severity level s or greater due to exposure for T hours is q ($0 < q < 1$). As an example, suppose T = 100 days and q = 0.10. The ERC_{10} is the dose for which the probability of an adverse effect of level s or higher due to exposure of 100 days is 0.10.

Duration of exposure and tissue dose (see Tables 1 and 2, respectively) in each selected study are used as predictor variables to establish the relationship between toxicity and globus pallidus Mn concentration at the end of exposure. In the *CatReg* interface, the logarithm (base ten) transformation was selected for both dose and duration of exposure to obtain the best fit (as guided by model's p-value and R^2 statistic). The two predictor variables are thus defined as

$$x_{i1} = log_{10}(EoE\ Globus\ Pallidus\ Mn\ concentration)$$

and

$$x_{i2} = log_{10}(Duration\ of\ Exposure).$$

Each exposure group (see Table 1) received a single severity score (SS) corresponding to the highest SS assigned for any significant outcome in that group. Fitting a categorical regression model in the traditional sense with multiple levels of severity was challenging in this application: sufficient data is needed to populate each severity level and, quite often, the literature is unable to support a complex severity scoring matrix. A multi-level matrix for scoring the severity of Mn health effects was developed and described by Mattison et al. (2017). Rather than focusing on a multi-level severity score scheme, a binary scheme was used in the present analysis, as was done by Milton et al. (2016) in their

Table 2
Summary of selected epidemiological studies.

Study[a]	Setting[b]	Size (N)[c]	TOTAL MnA[d] (μg/m^3)	RESP MnA[e] (μg/m^3)	Duration (years)	Sampling[f]	Significant Outcomes[g]	SS[h]
Bast-Pettersen et al. (2004), Ellingsen et al. (2003a), Ellingsen et al. (2003b)	FeMn and SiMn alloy plants	100 vs 100	AM 753 GM 301 Range 9–11457	AM 64 GM 36 Range 3–356 R/I 10.6%	AM 20 Range 2.1–41	Personal	Motor function and tremor (Static steadiness and tremor frequency test).	6
Lucchini et al. (1999), Lucchini et al. (1995)	FeMn Alloy plant	61 vs 87	AM 176 GM 54 Range 5–1490	AM 67 GM 17 Range 1–670 R/T 40–60%	GM 15.7	Both	Irritability, equilibrium loss, difficulty to direct to a fixed point on the first questionnaire; Tremor analysis, Motor function tests; Cognitive function tests.	6
Bouchard et al. (2007a), Bouchard et al. (2007b), Bouchard et al. (2008), Mergler et al. (1994)	FeMn and SiMn alloy facility	74 vs 74	AM 1186 GM 225 Range 14–11480	AM 122 GM 35 Range 1–1273 R/T 12–35%	16.7 (±3.2)	Stationary	Motor function tests; Cognitive function tests; Neuromotor, musculoskeletal and sensory symptoms; Mood states.	6
Myers et al. (2003a), Myers et al. (2003b), Young et al. (2005)	FeMn and FeSi alloy plants	509 vs 67	AM 800 GM 300 Range 0–5100	Median 58 Range 3–510 R/I NR	18.2 (±7.6)	Personal	Some "weak and unconvincing evidence for exposure effects" was found – "essentially a negative study"	0
Ellingsen et al. (2006), Ellingsen et al. (2008)	Shipyard welders	120 vs 96	AM 238 GM 121 Range 7–2322	NR R/T ~100%	AM 13.5 Range 1–40	Personal	Cognitive function and Motor function tests (finger tapping, foot tapping tests etc.).	6
Bowler et al. (2007a), Bowler et al. (2007b), Park et al. (2009)	Bay Bridge welders	43 vs NO	AM 210 Range 10–380	NR R/T NR	AM 16.5 months Range 6–28 months	Both	UPRDS scoring, bradykinesia, and several cases of manganism; hand tremor test; clinical depression and anxiety; Cognitive tests and Motor function tests.	7
Roels et al. (1992)	A dry alkaline battery plant	92 vs 101	AM 1780 GM 948 Range 46–10840	AM 301 GM 215 Range 21–1317 R/T NR	AM 5.3 Range 0.2–17.7	Personal	Simple visual reaction time, eye-hand coordination, hole tremor meter test, and audio verbal short-term memory test.	6
Gibbs et al. (1999)	Mn metal production facility	75 vs 75	AM 180 GM 110 Range 28–800	AM 66 GM 36 Range 5–230 R/T NR	AM 12.72 (±9.85)	Personal	No significant differences in any outcomes assessed, compared to controls.	0

Abbreviations: AM = Arithmetic Mean; GM = Geometric Mean; R/T or R/I = Respirable fraction in Total or Inhalable dust, respectively; NR = Not Reported; SS = Severity Score.
[a] Publications associated with this Study.
[b] Occupational setting.
[c] Number of subjects – exposed vs unexposed – Bowler et al. (2007b) study had no control group.
[d] Mn concentration measured in total dust – except for Ellingsen et al. and Myers et al. study that reported Mn measurements in inhalable dust.
[e] Mn concentration measured in respirable dust, as reported – along with respirable fraction, as reported.
[f] Type of samplers used for air Mn measurement – personal or stationary or both.
[g] Neurological outcomes that were reported as statistically significantly different in exposed group compared to unexposed groups.
[h] Maximum severity score assigned to the exposure group.

analysis of a copper toxicity database. Health outcomes scored 0, 1, or 2 are re-labelled as '0,' while outcomes scored greater than or equal to '3' are re-labelled as '1.' Therefore, the response variable (Y) for the categorical regression analysis is

$$Y_i = \begin{cases} 0 \; if \; S \leq 2 \\ 1 \; if \; S > 2 \end{cases}$$

The probability of a severity score greater than or equal to two (e.g. Y_i-1), predicted by the logarithm base ten transformed tissue dose and duration of exposure, is expressed as:

$$P(Y_i = 1) = \frac{\exp(\beta_0 + \beta_1 x_{i1} + \beta_{i2} x_{i2})}{1 + \exp(\beta_0 + \beta_1 x_{i1} + \beta_{i2} x_{i2})}$$

3. Results and discussion

3.1. Study selection and severity scoring

As establishing a relationship between dose and neurological outcome was the main goal of the current analysis, only peer-reviewed articles that had well documented air monitoring data and characterization of associated clinical outcomes were included. Most of these studies were also independently selected for use in the derivation of occupation exposure limits by regulatory authorities. A summary of the studies used in the current analysis is provided in Table 2. In all these studies except Bowler et al. (2007b), clinical outcomes in an exposed group were compared with those in an unexposed control or referent group.

Neurological outcomes (as reported in the original publication) from each study were evaluated using the 9-point severity scoring system developed by Mattison et al. (2017), with SS = 0 corresponding to a homeostatic response and SS = 9 representing a fatal outcome. Scoring of neurological outcomes (only those that were reported as statistically significantly different in exposed compared to referent or unexposed group) was performed by a group of scientists with expertise in toxicology, epidemiology and medicine. A list of health outcomes assessed attributed to the exposures in each group and the maximum severity score assigned to each exposure are shown in Table 2.

3.2. Testing PBPK model results against measured human blood Mn

The ability to appropriately predict the tissue Mn levels measured in epidemiological studies provides biological confirmation of the structure and parameterization of the PBPK model. The validation of the PBPK model against the empirical data is crucial for its application in risk assessment (WHO/IPCS, 2010). A PBPK model that compares well with empirical data allows researchers more confidence in predicting Mn concentrations in critical, though inaccessible tissues such as brain.

In general, comparison of PBPK models predictions against experimental values of internal dose relevant to risk assessment would be preferred. However, in the current context, comparison of PBPK model against human globus pallidus Mn concentration data was not be feasible due to the lack of appropriate data in the literature. Alternatively, blood Mn concentrations are reported in several human Mn exposure studies; therefore, as a pragmatic approach, blood Mn data was used as the tissue of choice to test the performance of model simulations against measured Mn levels.

Based on several studies involving welders, ferroalloy smelter workers and battery workers, whole blood Mn (MnB) appears to be a relatively good indicator of current (ongoing) exposures and can be used to distinguish exposed from unexposed subjects (Baker et al., 2014; Smith et al., 2007; Zheng et al., 2011). It is emphasized that these PBPK models in rats and monkeys were developed based on extensive PK data from a variety of tissues for many exposure conditions. The model behaviour was not developed based on the ability to predict or simulate blood Mn; however, all tissues in the model were connected by a blood compartment that had predicted Mn concentrations.

Visual inspection of model simulations shown in Fig. 2 indicates that the model-predicted MnB data is within the range of measured MnB values, with model output adequately reproducing the positive association observed between measured MnA and MnB values across all three studies. It's important to note that for a given dose, inter-subject variation in MnB exists; the current PBPK model cannot reflect these differences, but predicts an average dose-response relationship for the exposure situation in individuals with a specific set of parameter values.

Additionally, Schroeter et al. (2011) have shown that the PBPK model appropriately simulates whole body Mn tracer kinetics data of Mahoney and Small (1968) and plasma concentration data of humans receiving variable Mn diets from Freeland-Graves (1994) study. In summary, these findings indicate that the behaviour of the current Mn PBPK model should be adequate for tissue dose estimation from the human studies.

3.3. Modeling of selected studies and prediction of globus pallidus tissue doses

All selected studies were successfully simulated and tissue doses at the end of exposures (EoE) predicted. A summary of study-wise exposure conditions and model-derived tissue concentrations (EoE MnGP) is provided in Table 3. Key considerations or assumptions in modeling of these studies are discussed below.

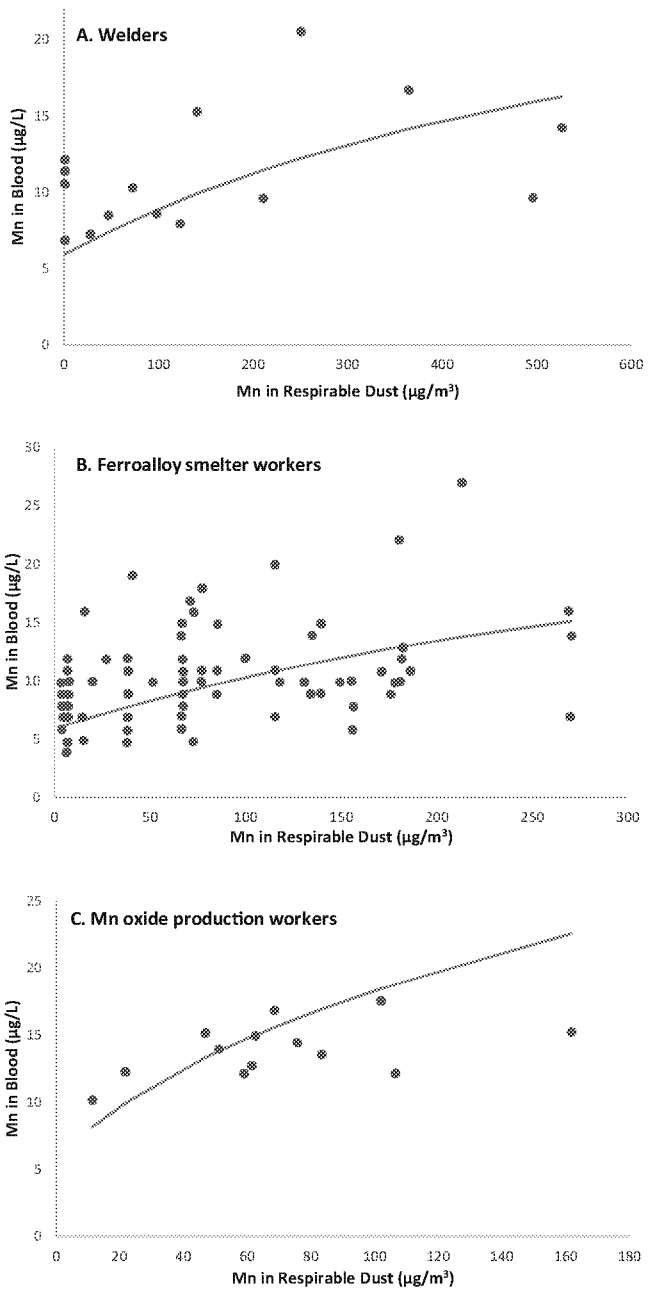

Fig. 2. Comparison of PBPK-model predictions (lines represent simulations based on data provided by authors of the cited studies) with measured blood manganese concentrations (as reported by the author of cited study) in welders: Figure A – simulations based on mean MnA and exposure duration data of Baker et al. (2014), ferroalloy smelter workers: Figure B – based on individual MnA data of Apostoli et al. (2000) and Mn oxide salt production workers: Figure C – based on mean MnA data of Roels et al. (1987). In these simulations, respirable fractions were 100% (according to Pesch et al. (2012)), 35–50% (as per original study) and 25% (assumed), respectively, of total dust. Note that for a given Mn exposure, inter-subject variation in MnB does exist; however, the current PBPK model cannot reflect these differences because it is deterministic. The Mn PBPK model predicts an average dose-response relationship for the exposure situation in individuals with a specific set of parameter values.

Note that the study-specific model input values were entered as group level data, with each value, being an aggregation of the whole group. Consequently, the resultant tissue dose value applies to the group, not to each subject. This approach is consistent with that used during severity scoring of study outcomes (Mattison

Table 3
Summary of model inputs and estimated globus pallidus Mn concentrations of each selected epidemiological study.

Key Study	Exposure Duration (years)[a]	Fraction (%) of Inhaled Dust deposited in Head[b]	Fraction (%) of Inhaled Dust deposited in Lungs[c]	Mn conc. in Respirable Dust (Resp MnA) (μg/m^3)[d]	End of Exposure Mn conc. in Globus Pallidus (EoE MnGP) (μg/g wet tissue)
Model Parameter:	*DSTOP*	*FDEPNO & FDEPNR*	*FDEPLU*	*DINH*	*CTOTST*
Bast-Pettersen et al. (2004)	20.2	61.8%	11%	64	0.532
Lucchini et al. (1999)	15.7	61.8%	11%	67	0.537
Mergler et al. (1994)	16.7	61.8%	11%	122	0.612
Young et al. (2005)	18.2	61.8%	11%	58	0.522
Ellingsen et al. (2008)[e]	13.5	21.1% or 24.5%	29.8% or 21.7%	238	0.671
Bowler et al. (2007b)[e]	1.375	21.1% 24.5%	29.8% 21.7%	190	0.63
Roels et al. (1992)	5.3	82.4%	8.2%	301	0.809
Gibbs et al. (1999)[f]	12.7	82.4%	8.2%	66	0.558

[a] Total number of exposure days were entered as exposure duration input; exposure duration is the difference between start of exposure (DSTART; DSTART = 100 was set to run the model for an 'acclimatization period' of 100 days with subjects only on diet and no inhalation exposure) and end of exposure (DSTOP) – also, for all simulations, exposure days per week (DAYSON = 5), h of exposure per day (TLEN = 8) were used.
[b] MPPD model output of head deposition fraction – this fraction was divided to olfactory fraction (FDEPNO) and respiratory fraction (FDEPNR) by 95:5 ratio (Schroeter et al., 2011).
[c] Sum of estimated pulmonary and tracheobronchial deposition fractions.
[d] Arithmetic mean Mn concentration in respirable dust, as reported – for welder studies, 100% welding dust considered as respirable (Pesch et al., 2012).
[e] Types of welding fumes reported for both Ellingsen et al. (2008) and Bowler et al. (2007b) study welders were shielded metal arc welding (SMAW) and flux-cored arc welding (FCAW) – therefore average of tissue doses estimated based on both types of PSD were used.
[f] Task/occupation-specific PSD data for Gibbs et al. (1999) study subjects was unavailable, thus deposition fractions of battery workers was assumed.

et al., 2017). In the severity scoring exercise, a single severity score was determined based on the mean response of an exposure group rather than on individual response, and the same response is assigned to the entire group. Use of individual exposure data rather than group level data for predicting tissue Mn levels, and combining them with individual response data, would improve confidence in dose-response analysis results. However, individual level quantitative information in the selected studies was unavailable.

Across all studies, average exposures of a group were reported as arithmetic (AM) and/or geometric mean (GM). Since use of AMs for characterizing the average exposure of a group is recommended over GMs for dose-response analysis purposes (Crump, 1998), we estimated target tissue concentrations in the globus pallidus associated only with reported arithmetic mean Mn concentrations of each exposure group.

The estimated MnGP in unexposed groups was 0.4 μg/g; this value represents that achieved with a constant exposure to background oral intake of 3 mg Mn/day in the absence of Mn inhalation.

Model simulations showed a half-time of approach to the new steady state of about 40 days. Resulting from the simulated inhalation exposure scenario (8hr/day, 5 days/week), a pattern of within-week (day-to-day) variation in tissue Mn levels was

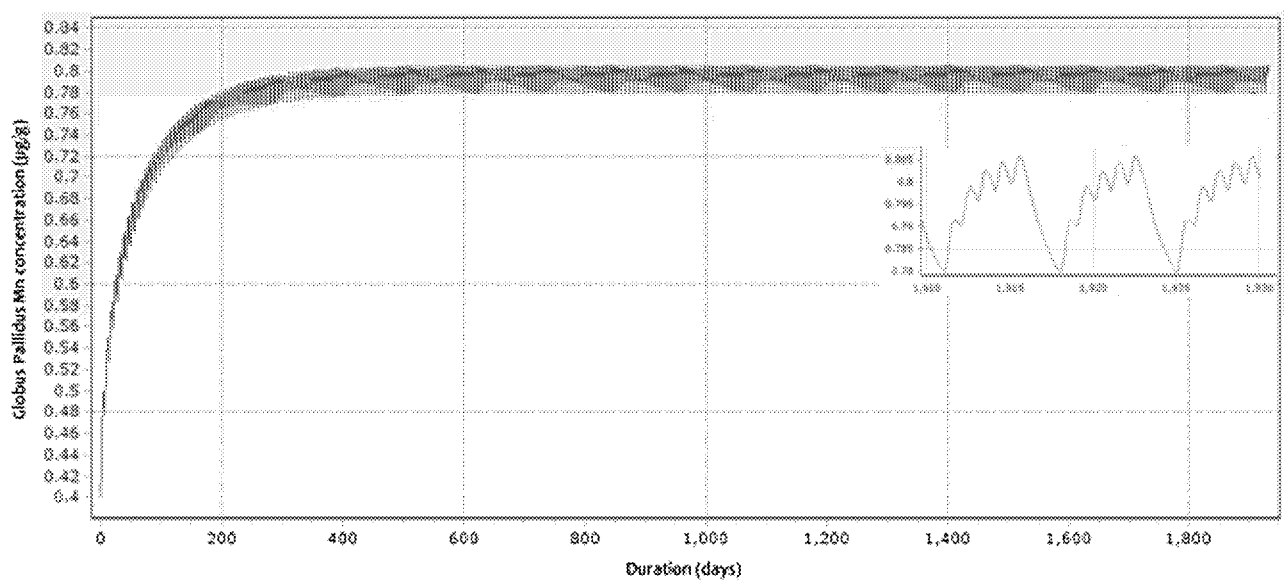

Fig. 3. PBPK simulation of Mn concentration – time profile of globus pallidus in welders under an exposure scenario as reported in Roels et al. (1992) study. Model simulations (line) of Mn globus pallidus (MnGP in μg/g) concentration in battery production workers exposed to Mn via inhalation (301 μg Mn/m^3 air for 8 h per day and 5 days per week) and via diet (3 mg Mn in diet per day; continuous exposure) for a period of 5.3 years. The inset picture shows the repeated within-week (day-to-day) variation in tissue Mn levels after reaching steady-state.

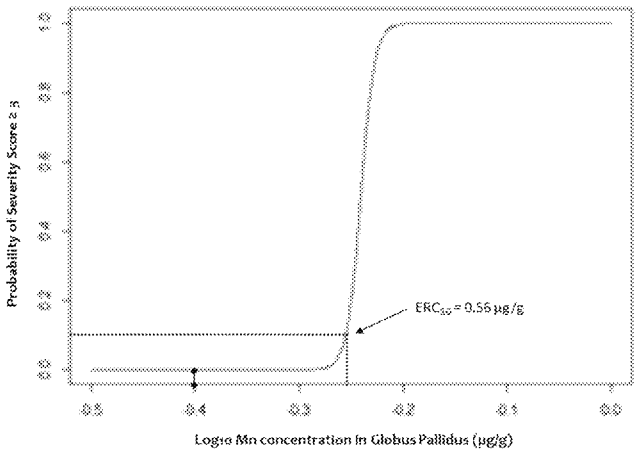

Fig. 4. Tissue dose – response relationship (CatReg model) of neurological outcomes based on selected Mn epidemiological studies using globus pallidus Mn (MnGP) as predictor variable. The CatReg model is shown with MnGP corresponding to an extra risk of 10% (ERC_{10}), after 5 years of exposure. The vertical line (continuous) corresponds to the PBPK model-estimated MnGP (0.4 µg/g) under a constant exposure to background oral intake of 3 mg Mn/day in the absence of Mn inhalation.

observed, as shown in Fig. 3. Therefore, to be consistent across all studies, simulations were designed to end on the same day of week (specifically, the 5th day of week).

3.4. Tissue Dose-Response Analysis (CatReg models)

Categorical regression analysis of severity scores assigned to neurological outcomes from eight epidemiological studies resulted in a steep dose-response curve (Fig. 4). The model deviance, tested with an F-statistic, provided a p-value of 0.002, indicating there is some relationship between the response and the tissue dose. Moreover, $R^2 = 0.65$, indicating that 65% of the variation in the data is explained by the model.

It is possible to evaluate the *CatReg* models for any number of years exposed. For the present analysis, to align with Health Canada's approach, *CatReg* models were evaluated with 5 years of exposure duration. Health Canada's report on human health risk assessment of inhaled Mn (HC, 2010) is based on dose-response assessment of data of an Italian ferroalloy workers study (Lucchini et al., 1999). HC (2010) used two exposure metrics: *"1) work history average respirable manganese (ARE); and 2) average respirable manganese over the five years prior to testing (ARE5). ARE5 was investigated based on biological evidence of the clearance of manganese from the brain over months to several years . . . ."*.

The ERC_{10} value of 0.55 µg/g may serve as a point of departure for establishing a reference concentration (RfC) for Mn. The dose-response curve below ERC_{10} is within the flat part of concentration-response relationship where Mn concentrations in the globus pallidus are essentially constant across the wide range of Mn exposures. Therefore, an adjustment factor of as little as 10-fold would be adequate to obtain an RfC.

3.5. Tissue dose based risk assessment

The experimental animal studies and occupational human studies strongly suggest a link between increased Mn concentrations in brain (specifically in globus pallidus) and reported subclinical or clinical neurological outcomes in exposed subjects. In the present analysis, this relationship has been explored for Mn risk assessment. To date, several human occupational studies were evaluated to assess the neurological outcomes associated with exposure to Mn through inhalation. Various regulatory authorities (WHO, US EPA, California OEHHA, and ATSDR) relied on a single study by Roels et al. (1992) for derivation of a point of departure and calculation of an inhalation reference value; Health Canada used the study by Lucchini et al. (1999) for this purpose. In contrast, rather than using data from only a single study, our

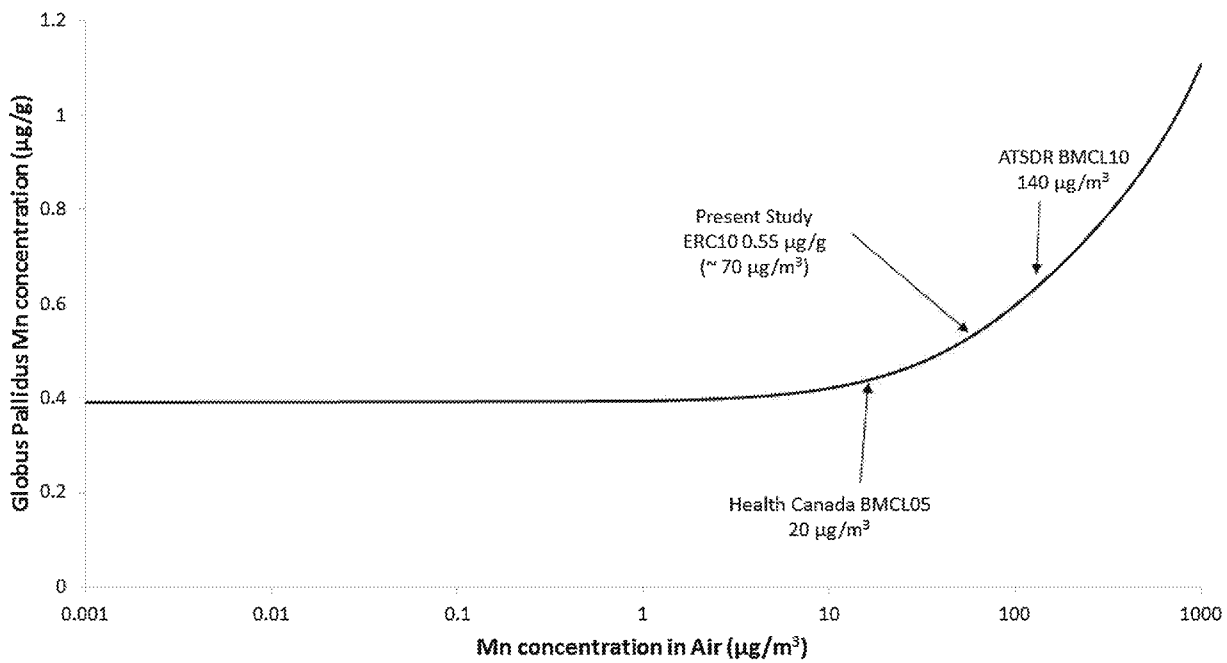

Fig. 5. Predicted globus pallidus Mn concentrations following exposure to 0–1000 µg Mn/m3 in air for 8 h/day, 5 d/week up to 5 years. The shaded region represents background MnGP range based on human autopsy reports of 'healthy' subjects. Also shown are PODs used by ATSDR (2012) and Health Canada (HC, 2010) in derivation of minimum risk level (MRL) and reference concentration (RfC), respectively.

concentration-response model was derived using data from multiple studies of Mn neurotoxicity. This model led to an estimate of ERC_{10} of 0.55 μg/g. Further, since Mn is an essential element necessary for proper functioning of every tissue including brain, the question of the range of Mn concentrations found in globus pallidus of healthy individuals and how the threshold compares to that range was explored. In the PBPK model, basal globus pallidus Mn concentration was set at 0.39 μg/g. However, due to the high variation in Mn dietary intake reported in human populations (0.7–10 mg/day, according to ATSDR (2012) and WHO (2011)), considerable variability in background globus pallidus tissue Mn levels is possible. In order to estimate this background range, a literature search was conducted to identify post-mortem studies which measure tissue Mn concentrations. Evaluation of several autopsy studies reporting MnGP measured in 'healthy' individuals indicates that this range lies between 0.24–0.64 μg/g (AndrăSI et al., 1990; Bush et al., 1995; Goldberg and Allen, 1981; Klos et al., 2006; Krebs et al., 2014; Layrargues et al., 1995; Maeda et al., 1997; Tracqui et al., 1995). This exercise suggests that ERC_{10} Mn concentration in the globus pallidus for adverse neurological outcomes derived in the present analysis is within the 'healthy' range and gives increased confidence in our findings. Furthermore, these results are consistent with a similar analysis done in non-human primates (Schroeter et al., 2012). Schroeter et al. (2012) simulated exposure scenarios from a large number of studies on monkeys exposed to Mn by various dose routes, exposure concentrations and durations and predicted the corresponding concentrations in the globus pallidus using a PBPK model for non-human primates. The reported responses were categorized using a clinical severity scoring system to allow for dose-response analysis. Using CatReg, an peak concentration ERC_{10} of 0.8 μg/g manganese in the globus pallidus was derived for a mild response comparable to subclinical effects measured in human occupational studies (Schroeter et al., 2012).

The PBPK model was further used to understand the air Mn concentrations associated with the MnGP ERC_{10} in a typical worker. To this end, a typical worker was as a 70 kg man exposed continuously to 3 mg/day dietary Mn and intermittently to $MnSO_4$ (particles which are highly soluble in mucus and tissue). The airway deposition fractions were 66% in head and 14% in lungs – based on Schroeter et al. (2011) with inhalation for 8 h/day, 5 d/week. The MnGP versus increasing air Mn concentrations (Fig. 5) shows the inhaled Mn for increasing MnGP to 0.55 μg/g is 70 μg Mn/m^3. For comparison, points of departure derived by Health Canada and ATSDR in the US are indicated on the same plot.

4. Conclusion

Blood Mn concentrations predicted by the PBPK model discussed in this manuscript fall within the range of blood Mn measured in human studies. Using this multi-species PBPK model, we simulated the increase in tissue Mn concentration over time in Mn industry workers in various studies. To take into account the effect of size of inhaled particles on lung deposition stemming from different types of industry, occupation-specific PSD was used in tissue dose predictions. Based on Mn exposure data from eight epidemiological studies and in conjunction with severity scores assigned to neurological outcomes, a tissue dose-response relationship was developed. This analysis is the first of its kind, providing a multi-study-based dose-response analysis of tissue Mn concentrations associated with neurological outcomes in humans. This analysis suggests that the globus pallidus Mn concentrations associated with a 10% extra risk of producing any adverse neurological responses in humans is 0.55 μg/g. Air Mn level associated with this pallidal Mn concentration is about 70 μg Mn/m^3 under occupational settings. With further refinement of the current dose-response relationship models, air Mn levels associated with the tissue dose ERC_{10} could be useful in setting or updating regulatory standards.

Acknowledgement

This work was funded by the International Manganese Institute. Daniel Krewski is the Natural Sciences and Engineering Research Council of Canada Chair in Risk Science at the University of Ottawa.

References

ATSDR, 2012. Agency for Toxic Substances and Disease Registry (ATSDR) Toxicological Profile for Manganese. ATSDR, Atlanta (GA) http://www.atsdr.cdc.gov/toxprofiles/tp151.pdf (Accessed 13 April 2016).

Andersen, M.E., Dorman, D.C., Clewell 3rd, H.J., Taylor, M.D., Nong, A., 2010. Multi-dose-route, multi-species pharmacokinetic models for manganese and their use in risk assessment. J. Toxicol. Environ. Health A 73 (2), 217–234.

AndrăSI, E., Nádasdi, J., Molnar, Z., Bezur, L., Ernyei, L., 1990. Determination of main and trace element contents in human brain by NAA and ICP-AES methods. In: Zeisler, R., Guinn, V.P. (Eds.), Nuclear Analytical Methods in the Life Sciences. Humana Press, Totowa, Nj, pp. 691–698.

Anjilvel, S., Asgharian, B., 1995. A multiple-path model of particle deposition in the rat lungFundam. Appl. Toxicol.: Off. J. Soc. Toxicol. 28 (1), 41–50. . (Available at) https://www.ara.com/products/multiple-path-particle-dosimetry-model-mppd-v-211.

Apostoli, P., Lucchini, R., Alessio, L., 2000. Are current biomarkers suitable for the assessment of manganese exposure in individual workers? Am. J. Ind. Med. 37 (3), 283–290.

Aschner, J.L., Aschner, M., 2005. Nutritional aspects of manganese homeostasis. Mol. Aspects Med. 26 (4–5), 353–362.

Aschner, M., Guilarte, T.R., Schneider, J.S., Zheng, W., 2007. Manganese: recent advances in understanding its transport and neurotoxicity. Toxicol. Appl. Pharmacol. 221 (2), 131–147.

Aschner, M., Erikson, K.M., Herrero Hernandez, E., Tjalkens, R., 2009. Manganese and its role in Parkinson's disease: from transport to neuropathology. Neuromol. Med. 11 (4), 252–266.

Asgharian, B., Hofmann, W., Bergmann, R., 2001. Particle deposition in a multiple-path model of the human lung. Aerosol Sci. Technol. 34 (4), 332–339.

Baker, M.G., Simpson, C.D., Stover, B., Sheppard, L., Checkoway, H., Racette, B.A., Seixas, N.S., 2014. Blood manganese as an exposure biomarker: state of the evidence. J. Occup. Environ. Hyg. 11 (4), 210–217.

Bast-Pettersen, R., Ellingsen, D.G., Hetland, S.M., Thomassen, Y., 2004. Neuropsychological function in manganese alloy plant workers. Int. Arch. Occup. Environ. Health 77 (4), 277–287.

Berlinger, B., Benker, N., Weinbruch, S., L'Vov, B., Ebert, M., Koch, W., Ellingsen, D.G., Thomassen, Y., 2011. Physicochemical characterisation of different welding aerosols. Anal. Bioanal. Chem. 399 (5), 1773–1780.

Bouchard, M., Mergler, D., Baldwin, M., Panisset, M., Bowler, R., Roels, H.A., 2007a. Neurobehavioral functioning after cessation of manganese exposure: a follow-up after 14 years. Am. J. Ind. Med. 50 (11), 831–840.

Bouchard, M., Mergler, D., Baldwin, M., Panisset, M., Roels, H.A., 2007b. Neuropsychiatric symptoms and past manganese exposure in a ferro-alloy plant. Neurotoxicology 28 (2), 290–297.

Bouchard, M., Mergler, D., Baldwin, M.E., Panisset, M., 2008. Manganese cumulative exposure and symptoms: a follow-up study of alloy workers. Neurotoxicology 29 (4), 577–583.

Bowler, R.M., Gysens, S., Diamond, E., Nakagawa, S., Drezgic, M., Roels, H.A., 2006. Manganese exposure: neuropsychological and neurological symptoms and effects in welders. Neurotoxicology 27 (3), 315–326.

Bowler, R.M., Nakagawa, S., Drezgic, M., Roels, H.A., Park, R.M., Diamond, E., Mergler, D., Bouchard, M., Bowler, R.P., Koller, W., 2007a. Sequelae of fume exposure in confined space welding: a neurological and neuropsychological case series. Neurotoxicology 28 (2), 298–311.

Bowler, R.M., Roels, H.A., Nakagawa, S., Drezgic, M., Diamond, E., Park, R., Koller, W., Bowler, R.P., Mergler, D., Bouchard, M., Smith, D., Gwiazda, R., Doty, R.L., 2007b. Dose-effect relationships between manganese exposure and neurological, neuropsychological and pulmonary function in confined space bridge welders. Occup. Environ. Med. 64 (3), 167–177.

Bush, V.J., Moyer, T.P., Batts, K.P., Parisi, J.E., 1995. Essential and toxic element concentrations in fresh and formalin-fixed human autopsy tissues. Clin. Chem. 41 (2), 284–294.

Cersosimo, M.G., Koller, W.C., 2006. The diagnosis of manganese-induced parkinsonism. Neurotoxicology 27 (3), 340–346.

Chang, Y., Woo, S.T., Kim, Y., Lee, J.J., Song, H.J., Lee, H.J., Kim, S.H., Lee, H., Kwon, Y.J., Ahn, J.H., Park, S.J., Chung, I.S., Jeong, K.S., 2010. Pallidal index measured with three-dimensional T1-weighted gradient echo sequence is a good predictor of manganese exposure in welders. J. Magn. Reson. Imaging: JMRI 31 (4), 1020–1026.

Chen, P., 2015. Age- and manganese-dependent modulation of dopaminergic phenotypes in a C elegans Dj-1 genetic model of Parkinson's disease. Metallomics 7 (2), 289–298.

Chen, P., Chakraborty, S., Mukhopadhyay, S., Lee, E., Paoliello, M.M., Bowman, A.B., Aschner, M., 2015. Manganese homeostasis in the nervous system. J. Neurochem. 134 (4), 601–610.
Cotzias, G.C., Horiuchi, K., Fuenzalida, S., Mena, I., 1968. Chronic manganese poisoning. Clearance of tissue manganese concentrations with persistance of the neurological picture. Neurology 18 (4), 376–382.
Crossgrove, J., Zheng, W., 2004. Manganese toxicity upon overexposure. NMR Biomed. 17 (8), 544–553.
Crump, K.S., 1998. On summarizing group exposures in risk assessment: is an arithmetic mean or a geometric mean more appropriate? Risk Anal.: Off. Publ. Soc. Risk Anal. 18 (3), 293–297.
Davis, C.D., Zech, L., Greger, J.L., 1993. Manganese metabolism in rats: an improved methodology for assessing gut endogenous losses. Proceedings of the Society for Experimental Biology and Medicine. Soc. Exp. Biol. Med. (New York, N.Y.) 202 (1), 103–108.
DeWitt, M.R., Chen, P., Aschner, M., 2013. Manganese efflux in Parkinsonism: insights from newly characterized SLC30A10 mutations. Biochem. Biophys. Res. Commun. 432 (1), 1–4.
Dorman, D.C., Struve, M.F., James, R.A., Marshall, M.W., Parkinson, C.U., Wong, B.A., 2001. Influence of particle solubility on the delivery of inhaled manganese to the rat brain: manganese sulfate and manganese tetroxide pharmacokinetics following repeated (14-day) exposure. Toxicol. Appl. Pharmacol. 170 (2), 79–87.
Dorman, D.C., McManus, B.E., Parkinson, C.U., Manuel, C.A., McElveen, A.M., Everitt, J.I., 2004. Nasal toxicity of manganese sulfate and manganese phosphate in young male rats following subchronic (13-week) inhalation exposure. Inhal. Toxicol. 16 (6–7), 481–488.
Dorman, D.C., Struve, M.F., Marshall, M.W., Parkinson, C.U., James, R.A., Wong, B.A., 2006. Tissue manganese concentrations in young male rhesus monkeys following subchronic manganese sulfate inhalation. Toxicol. Sci. 92 (1), 201–210.
Douglas, P.K., Cohen, M.S., DiStefano, J.J., 2010. Chronic exposure to Mn inhalation may have lasting effects: a physiologically-based toxicokinetic model in rats. Toxicol. Environ. Chem. 92 (2), 279–299.
Ellingsen, D.G., Haug, E., Gaarder, P.I., Bast-Pettersen, R., Thomassen, Y., 2003a. Endocrine and immunologic markers in manganese alloy production workers. Scand. J. Work, Environ. Health 29 (3), 230–238.
Ellingsen, D.G., Haug, E., Ulvik, R.J., Thomassen, Y., 2003b. Iron status in manganese alloy production workers. J. Appl. Toxicol.: JAT 23 (4), 239–247.
Ellingsen, D.G., Dubeikovskaya, L., Dahl, K., Chashchin, M., Chashchin, V., Zibarev, E., Thomassen, Y., 2006. Air exposure assessment and biological monitoring of manganese and other major welding fume components in welders. J. Environ. Monit.: JEM 8 (10), 1078–1086.
Ellingsen, D.G., Konstantinov, R., Bast-Pettersen, R., Merkurjeva, L., Chashchin, M., Thomassen, Y., Chashchin, V., 2008. A neurobehavioral study of current and former welders exposed to manganese. Neurotoxicology 29 (1), 48–59.
Finley, J.W., Johnson, P.E., Johnson, L.K., 1994. Sex affects manganese absorption and retention by humans from a diet adequate in manganese. Am. J. Clin. Nutr. 60 (6), 949–955.
Freeland-Graves, J., 1994. Derivation of manganese estimated safe and adequate daily dietary intakes. Risk Assess. Essent. Elem. 237–252.
Gibbs, J.P., Crump, K.S., Houck, D.P., Warren, P.A., Mosley, W.S., 1999. Focused medical surveillance: a search for subclinical movement disorders in a cohort of U.S. workers exposed to low levels of manganese dust. Neurotoxicology 20 (2–3), 299–313.
Goldberg, W.J., Allen, N., 1981. Determination of Cu, Mn, Fe, and Ca in six regions of normal human brain, by atomic absorption spectroscopy. Clin. Chem. 27 (4), 562–564.
Guilarte, T.R., 2010. Manganese and Parkinson's disease: a critical review and new findings. Environ. Health Perspect. 118 (8), 1071–1080.
Gunier, R., Jerrett, M., Smith, D., Jursa, T., Yousefi, P., Camacho, J., Hubbard, A., Eskenazi, B., Bradman, A., 2014. Determinants of manganese levels in house dust: samples from the CHAMACOS cohort. Sci. Total Environ. 497, 360–368.
Gunter, T.E., Gerstner, B., Gunter, K.K., Malecki, J., Gelein, R., Valentine, W.M., Aschner, M., Yule, D.I., 2013. Manganese transport via the transferrin mechanism. Neurotoxicology 34, 118–127.
HC, 2010. Human Health Risk Assessment for Inhaled Manganese. Health Canada, Ottawa, Ontario http://healthycanadians.gc.ca/publications/healthy-living-vie-saine/manganese/index-eng.php Accessed 13 April 2016).
ICRP, 1994. Human respiratory tract model for radiological protection. A report of a Task Group of the International Commission on Radiological Protection. Ann. ICRP 24 (1–3), 1–482.
IEH, 2004. Occupational Exposure Limits: Criteria Document for Manganese and Inorganic Manganese Compounds (Web Report W17). MRC Institute for Environment and Health, Leicester, UK http://www.iehconsulting.co.uk/IEH_Consulting/IEHCPubs/HumExpRiskAssess/w17.pdf Accessed 13 April 2016).
Iwami, O., Watanabe, T., Moon, C.-S., Nakatsuka, H., Ikeda, M., 1994. Motor neuron disease on the Kii Peninsula of Japan: excess manganese intake from food coupled with low magnesium in drinking water as a risk factor. Sci. Total Environ. 149 (1), 121–135.
Jarvisalo, J., Olkinuora, M., Kiilunen, M., Kivisto, H., Ristola, P., Tossavainen, A., Aitio, A., 1992. Urinary and blood manganese in occupationally nonexposed populations and in manual metal arc welders of mild steel. Int. Arch. Occup. Environ. Health 63 (7), 495–501.
Jenkins, N.T., Pierce, W.M.G., Eagar, T.W., 2005. Particle size distribution of gas metal and flux cored arc welding fumes. Weld. Res. 84 (10), 156s–163s.
Jiang, Y., Zheng, W., Long, L., Zhao, W., Li, X., Mo, X., Lu, J., Fu, X., Li, W., Liu, S., Long, Q., Huang, J., Pira, E., 2007. Brain magnetic resonance imaging and manganese concentrations in red blood cells of smelting workers: search for biomarkers of manganese exposure. Neurotoxicology 28 (1), 126–135.
Kim, E., Kim, Y., Cheong, H.-K., Cho, S., Shin, Y.C., Sakong, J., Kim, K.S., Yang, J.S., Jin, Y.-W., Kang, S.-K., 2005. Pallidal index on MRI as a target organ dose of manganese: structural equation model analysis. Neurotoxicology 26 (3), 351–359.
Klos, K.J., Chandler, M., Kumar, N., Ahlskog, J.E., Josephs, K.A., 2006. Neuropsychological profiles of manganese neurotoxicity. Eur. J. Neurol. 13 (10), 1139–1141.
Kondakis, X.G., Makris, N., Leotsinidis, M., Prinou, M., Papapetropoulos, T., 1989. Possible health effects of high manganese concentration in drinking water. Arch. Environ. Health: Int. J. 44 (3), 175–178.
Krebs, N., Langkammer, C., Goessler, W., Ropele, S., Fazekas, F., Yen, K., Scheurer, E., 2014. Assessment of trace elements in human brain using inductively coupled plasma mass spectrometry. J. Trace Elem. Med. Biol.: Organ Soc. Miner. Trace Elem. 28 (1), 1–7.
Layrargues, G.P., Shapcott, D., Spahr, L., Butterworth, R.F., 1995. Accumulation of manganese and copper in pallidum of cirrhotic patients: role in the pathogenesis of hepatic encephalopathy? Metab. Brain Dis. 10 (4), 353–356.
Leavens, T.L., Rae, D., Andersen, M.E., Dorman, D.C., 2007. Evaluating transport of manganese from olfactory mucosa to striatum by pharmacokinetic modeling. Toxicol. Sci. 97 (2), 265–278.
Li, S.J., Jiang, L., Fu, X., Huang, S., Huang, Y.N., Li, X.R., Chen, J.W., Li, Y., Luo, H.L., Wang, F., Ou, S.Y., Jiang, Y.M., 2014. Pallidal index as biomarker of manganese brain accumulation and associated with manganese levels in blood: a meta-analysis. PLoS One 9 (4), e93900.
Ljung, K., Vahter, M., 2007. Time to re-evaluate the guideline value for manganese in drinking water? Environ. Health Perspect. 1533–1538.
Lucchini, R., Selis, L., Folli, D., Apostoli, P., Mutti, A., Vanoni, O., Iregren, A., Alessio, L., 1995. Neurobehavioral effects of manganese in workers from a ferroalloy plant after temporary cessation of exposure. Scand. J. Work Environ. Health 21 (2), 143–149.
Lucchini, R., Apostoli, P., Perrone, C., Placidi, D., Albini, E., Migliorati, P., Mergler, D., Sassine, M.P., Palmi, S., Alessio, L., 1999. Long-term exposure to low levels of manganese oxides and neurofunctional changes in ferroalloy workers. Neurotoxicology 20 (2–3), 287–297.
Maeda, H., Sato, M., Yoshikawa, A., Kimura, M., Sonomura, T., Terada, M., Kishi, K., 1997. Brain MR imaging in patients with hepatic cirrhosis: relationship between high intensity signal in basal ganglia on T1-weighted images and elemental concentrations in brain. Neuroradiology 39 (8), 546–550.
Mahoney, J.P., Small, W.J., 1968. Studies on manganese: III. The biological half-life of radiomanganese in man and factors which affect this half-life. J. Clin. Invest. 47 (3), 643.
Malecki, E.A., Radzanowski, G.M., Radzanowski, T.J., Gallaher, D.D., Greger, J.L., 1996. Biliary manganese excretion in conscious rats is affected by acute and chronic manganese intake but not by dietary fat. J. Nutr. 126 (2), 489–498.
Mattison, D., Milton, B., Krewski, D., Levy, L., Dorman, D.C., Aggett, P.J., Roels, H., Andersen, M., Karyakina, N., Shilnikova, N., Ramoju, S., McGough, D., 2017. Severity scoring of manganese health effects for categorical regression. J. Neurol. Toxicol. 58, 203–216.
Mergler, D., Huel, G., Bowler, R., Iregren, A., Belanger, S., Baldwin, M., Tardif, R., Smargiassi, A., Martin, L., 1994. Nervous system dysfunction among workers with long-term exposure to manganese. Environ. Res. 64 (2), 151–180.
Milton, B., Farrell, P.J., Birkett, N., Krewski, D., 2016. Modeling U-shaped exposure-response relationships for agents that demonstrate toxicity due to both excess and deficiency. Risk Anal.: Off. Publ. Soc. Risk Anal..
Myers, J.E., Thompson, M.L., Naik, I., Theodorou, P., Esswein, E., Tassell, H., Daya, A., Renton, K., Spies, A., Paicker, J., Young, T., Jeebhay, M., Ramushu, S., London, L., Rees, D.J., 2003a. The utility of biological monitoring for manganese in ferroalloy smelter workers in South Africa. Neurotoxicology 24 (6), 875–883.
Myers, J.E., Thompson, M.L., Ramushu, S., Young, T., Jeebhay, M.F., London, L., Esswein, E., Renton, K., Spies, A., Boulle, A., Naik, I., Iregren, A., Rees, D.J., 2003b. The nervous system effects of occupational exposure on workers in a South African manganese smelter. Neurotoxicology 24 (6), 885–894.
Nong, A., Teeguarden, J.G., Clewell 3rd, H.J., Dorman, D.C., Andersen, M.E., 2008. Pharmacokinetic modeling of manganese in the rat IV: Assessing factors that contribute to brain accumulation during inhalation exposure. J. Toxicol. Environ. Health A 71 (7), 413–426.
Nong, A., Taylor, M.D., Clewell 3rd, H.J., Dorman, D.C., Andersen, M.E., 2009. Manganese tissue dosimetry in rats and monkeys: accounting for dietary and inhaled Mn with physiologically based pharmacokinetic modeling. Toxicol. Sci. 108 (1), 22–34.
Normandin, L., Carrier, G., Gardiner, P.F., Kennedy, G., Hazell, A.S., Mergler, D., Butterworth, R.F., Philippe, S., Zayed, J., 2002. Assessment of bioaccumulation, neuropathology, and neurobehavior following subchronic (90 days) inhalation in Sprague-Dawley rats exposed to manganese phosphate. Toxicol. Appl. Pharmacol. 183 (2), 135–145.
O'Neal, S.L., Zheng, W., 2015. Manganese toxicity upon overexposure: a decade in review. Curr. Environ. Health. Rep. 2 (3), 315–328.
Olanow, C.W., 2004. Manganese-induced parkinsonism and Parkinson's disease. Ann. N. Y. Acad. Sci. 1012, 209–223.
Park, R.M., Bowler, R.M., Roels, H.A., 2009. Exposure-response relationship and risk assessment for cognitive deficits in early welding-induced manganism. J. Occup. Environ. Med./Am. Coll. Occup. Environ. Med. 51 (10), 1125–1136.

Perl, D.P., Olanow, C.W., 2007. The neuropathology of manganese-induced Parkinsonism. J. Neuropathol. Exp. Neurol. 66 (8), 675–682.
Pesch, B., Weiss, T., Kendzia, B., Henry, J., Lehnert, M., Lotz, A., Heinze, E., Kafferlein, H.U., Van Gelder, R., Berges, M., Hahn, J.U., Mattenklott, M., Punkenburg, E., Hartwig, A., Bruning, T., 2012. Levels and predictors of airborne and internal exposure to manganese and iron among welders. J. Exposure Sci. Environ. Epidemiol. 22 (3), 291–298.
Post, J.E., 1999. Manganese oxide minerals: crystal structures and economic and environmental significance. Proc. Natl. Acad. Sci. 96 (7), 3447–3454.
Roels, H., Lauwerys, R., Genet, P., Sarhan, M.J., de Fays, M., Hanotiau, I., Buchet, J.P., 1987. Relationship between external and internal parameters of exposure to manganese in workers from a manganese oxide and salt producing plant. Am. J. Ind. Med. 11 (3), 297–305.
Roels, H.A., Ghyselen, P., Buchet, J.P., Ceulemans, E., Lauwerys, R.R., 1992. Assessment of the permissible exposure level to manganese in workers exposed to manganese dioxide dust. Br. J. Ind. Med. 49 (1), 25–34.
Roels, H.A., Ortega Eslava, M.J., Ceulemans, E., Robert, A., Lison, D., 1999. Prospective study on the reversibility of neurobehavioral effects in workers exposed to manganese dioxide. Neurotoxicology 20 (2–3), 255–271.
Salehi, F., Krewski, D., Mergler, D., Normandin, L., Kennedy, G., Philippe, S., Zayed, J., 2003. Bioaccumulation and locomotor effects of manganese phosphate/sulfate mixture in Sprague-Dawley rats following subchronic (90 days) inhalation exposure. Toxicol. Appl. Pharmacol. 191 (3), 264–271.
Schroeter, J.D., Nong, A., Yoon, M., Taylor, M.D., Dorman, D.C., Andersen, M.E., Clewell, H.J., 2011. Analysis of manganese tracer kinetics and target tissue dosimetry in monkeys and humans with multi-route physiologically based pharmacokinetic models. Toxicol. Sci. 120 (2), 481–498.
Schroeter, J.D., Dorman, D.C., Yoon, M., Nong, A., Taylor, M.D., Andersen, M.E., Clewell, H.J., 2012. Application of a multi-route physiologically based pharmacokinetic model for manganese to evaluate dose-dependent neurological effects in monkeys. Toxicol. Sci. 129 (2), 432–446.
Smith, D., Gwiazda, R., Bowler, R., Roels, H., Park, R., Taicher, C., Lucchini, R., 2007. Biomarkers of Mn exposure in humans. Am. J. Ind. Med. 50 (11), 801–811.
Tan, J., Zhang, T., Jiang, L., Chi, J., Hu, D., Pan, Q., Wang, D., Zhang, Z., 2011. Regulation of intracellular manganese homeostasis by kufor-Rakeb syndrome-associated ATP13A2 protein. J. Biol. Chem. 286 (34), 29654–29662.
Taylor, M.D., Clewell 3rd, H.J., Andersen, M.E., Schroeter, J.D., Yoon, M., Keene, A.M., Dorman, D.C., 2012. Update on a pharmacokinetic-Centric alternative tier II program for MMT-Part II: physiologically based pharmacokinetic modeling and manganese risk assessment. J. Toxicol. 2012, 791431.
Teeguarden, J.G., Dorman, D.C., Covington, T.R., Clewell 3rd, H.J., Andersen, M.E., 2007a. Pharmacokinetic modeling of manganese. I. Dose dependencies of uptake and elimination. J. Toxicol. Environ. Health A 70 (18), 1493–1504.
Teeguarden, J.G., Dorman, D.C., Nong, A., Covington, T.R., Clewell 3rd, H.J., Andersen, M.E., 2007b. Pharmacokinetic modeling of manganese. II. Hepatic processing after ingestion and inhalation. J. Toxicol. Environ. Health A 70 (18), 1505–1514.
Teeguarden, J.G., Gearhart, J., Clewell 3rd, H.J., Covington, T.R., Nong, A., Andersen, M.E., 2007c. Pharmacokinetic modeling of manganese. III. Physiological approaches accounting for background and tracer kinetics. J. Toxicol. Environ. Health A 70 (18), 1515–1526.
Tracqui, A., Tayot, J., Kintz, P., Alves, G., Bosque, M.A., Mangin, P., 1995. Determination of manganese in human brain samples. Forensic Sci. Int. 76 (3), 199–203.
USEPA, 1993. Manganese (CASRN 7439-96-5). Inhalation RfC Assessment, https://cfpub.epa.gov/ncea/iris/iris_documents/documents/subst/0373_summary.pdf#nameddest=rfc Accessed 13 April 2016).
USEPA, 2006. CatReg software for categorical regression analysis. U.S. Environmental Protection Agency, Office of Research and Development, National Center For Environmental Assessment. Research Triangle Park Office, Research Triangle Park, NC https://cfpub.epa.gov/si/si_public_record_report.cfm?dirEntryId=233029 Accessed 13 April 2016).
WHO, 2011. Manganese in drinking-water. Background Document for Preparation of WHO Guidelines for Drinking-water Quality. World Health Organization, Geneva (WHO/SDE/WSH/03.04/104/Rev/1) http://www.who.int/water_sanitation_health/dwq/chemicals/manganese.pdf Accessed 13 April 2016.
WHO/IPCS, 2010. Characterization and application of physiologically based pharmacokinetic models in risk assessment. World Health Organization, International Programme on Chemical Safety, Geneva, Switzerland http://www.who.int/ipcs/methods/harmonization/areas/pbpk_models.pdf (Accessed 13 April 2016).
Wang, X., Yang, Y., Wang, X., Xu, S., 2006. The effect of occupational exposure to metals on the nervous system function in welders. J. Occup. Health 48 (2), 100–106.
Young, T., Myers, J.E., Thompson, M.L., 2005. The nervous system effects of occupational exposure to manganese–measured as respirable dust–in a South African manganese smelter. Neurotoxicology 26 (6), 993–1000.
Zheng, W., Fu, S.X., Dydak, U., Cowan, D.M., 2011. Biomarkers of manganese intoxication. Neurotoxicology 32 (1), 1–8.